ATP-Mediated Changes in Cross-Subunit Interactions in the RecA Protein

Karen M. Logan, Anthony L. Forget, John Paul Verderese, and Kendall L. Knight*

Department of Biochemistry and Molecular Pharmacology, University of Massachusetts Medical School, 55 Lake Avenue North, Worcester, Massachusetts 01655-0103

Received May 25, 2001; Revised Manuscript Received July 18, 2001

ABSTRACT: RecA protein undergoes ATP- and DNA-induced conformational changes that result in different helical parameters for free protein filaments versus RecA/ATP/DNA nucleoprotein filaments. Previous mutational studies of a particular region of the RecA oligomeric interface suggested that cross-subunit contacts made by residues K6 and R28 were more important for stabilization of free protein oligomers than nucleoprotein filaments [Eldin, S., et al. (2000) *J. Mol. Biol. 299*, 91−101]. Using mutant proteins with specifically engineered Cys substitutions, we show here that the efficiency of cross-subunit disulfide bond formation at certain positions in this region changes in the presence of ATP or ATP/DNA. Our results support the idea that specific cross-subunit interactions that occur within this region of the subunit interface are different in free RecA protein versus RecA/ATP/DNA nucleoprotein filaments.

The bacterial RecA protein mediates genetic recombination by catalyzing strand exchange between DNAs of related sequence. In the presence of ATP, RecA binds to ssDNA with high affinity and it is this RecA/ATP/ssDNA nucleoprotein filament that is the catalytically active form of the protein (*1*−*4*). Recent studies have shown that ATP promotes high affinity ssDNA binding by increasing the cooperative association of subunits rather than by increasing the inherent affinity of monomeric RecA for ssDNA (*5*). Therefore, our studies of the oligomeric properties of RecA have involved the identification and characterization of residues within different regions of the interface that play important roles in the transmission of ATP-mediated allosteric information as well as in the stabilization of the oligomeric structure of the protein filament.

The present study focuses on an area of the interface defined by the N-terminal region of RecA in one subunit (residues 6−30) and the complementary interacting surface on the neighboring subunit defined by residues 111−140 (ref *6*; Figure 1). Early genetic studies using peptides consisting of the N-terminal 77 residues (*7*) or the N-terminal 50 residues (*8*) suggested that these formed mixed oligomers with wild-type RecA, thereby, inhibiting its activity. Subsequent biochemical studies demonstrated the importance of the N-terminal 33 residues for RecA self-assembly (*9*) and also supported the idea that folding of the N-terminal α-helix (residues 3−21) is coupled to RecA self-assembly (*10*). Although cross-subunit interactions in this region of the interface are largely hydrophobic, the RecA crystal structure shows the following cross-subunit ionic and polar interactions as well: K6↔D139, R28↔D112 and R28↔N113. Unexpectedly, we have found that mutations at K6 and R28 impose severe defects on the oligomeric stability of free RecA protein, whereas mutations at D112, N113, and D139 do not (*11*). However, K6 and R28 mutant proteins showed an apparent normal formation of nucleoprotein filaments and had nearly wild-type-like catalytic abilities. These results suggested that cross-subunit contacts made by K6 and R28 with positions in the neighboring subunit are different in the active vs inactive form of the protein.

In this study, we have created a series of mutant RecA proteins with pairwise Cys substitutions at positions 6/139, 28/112, and 28/113 to test the efficiency of disulfide bond formation under various conditions. Our data provide a direct demonstration of ATP-induced changes in cross-subunit interactions made between residues in this region of the subunit interface.

EXPERIMENTAL PROCEDURES

Plasmids and Proteins. Wild-type and all mutant *recA* genes are carried on plasmids in which *recA* expression is regulated by the *tac* promoter (*12*). Screens for in vivo function were carried out in either of two Δ*recA Escherichia coli* strains, MV1190 (*12*) or DE1663' (*13*). φX174 circular ssDNA was purchased from New England Biolabs, and RV-1 circular ssDNA was made as previously described (*14*). RecA proteins were purified using variations of a previously described procedure (*15*). All buffers used in purification of mutant proteins contained 20 mM βME to prevent spontaneous disulfide bond formation. Purification protocols were slightly different for each mutant protein and involved the use of one or more of the following chromatographic steps: ATP-agarose, heparin agarose, ceramic hydroxyapatite, Superose 6 gel filtration, or Sephacryl S-1000 gel filtration.

Mutagenesis. Amino acid substitutions were introduced using modifications of a previously described cassette mutagenesis procedure (*16*) or a PCR-based method (QuikChange; Stratagene).

In Vivo Activities of RecA Mutants. Assays for recombinational DNA repair involved measurements of cell survival

† This work was supported by NIH grant GM44772 to K.L.K. Its contents are the sole responsibility of the authors and do not necessarily represent the official views of the NIH.

* To whom correspondence should be addressed. Phone: (508) 856-2405. Fax: (508) 856-6231. E-mail: kendall.knight@umassmed.edu.

10.1021/bi011081u CCC: $20.00
Published on Web 08/28/2001

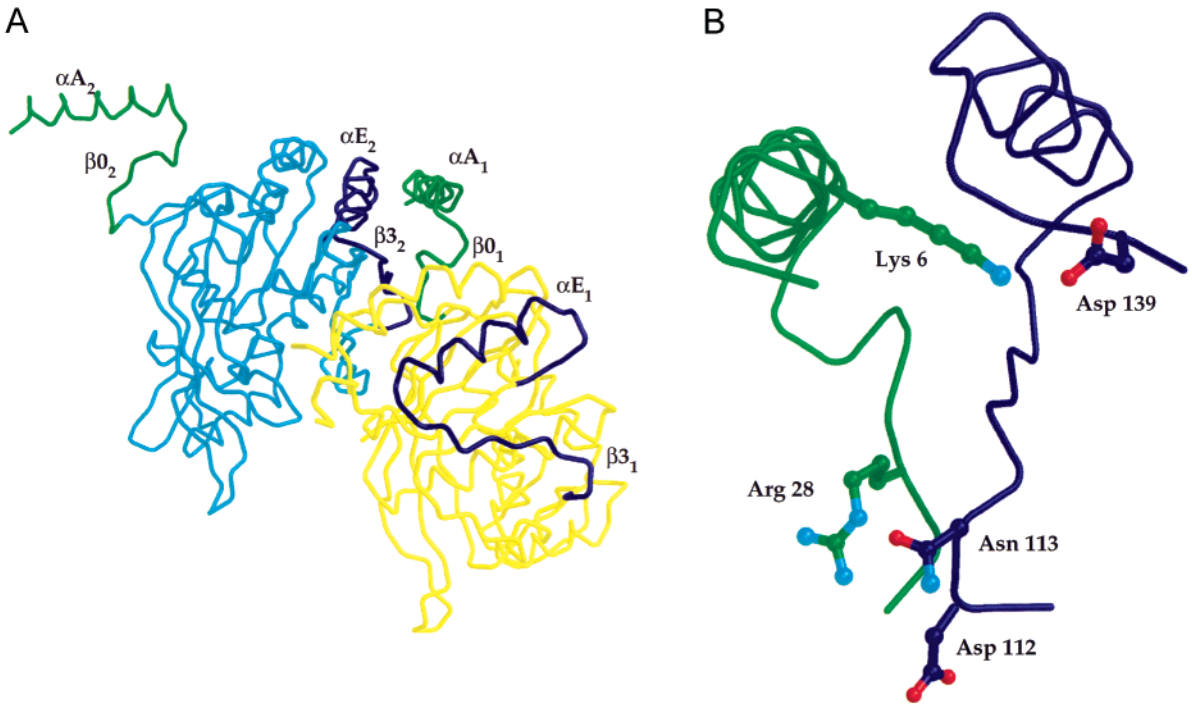

FIGURE 1: Details of the oligomeric interactions in this study. (A) An α-carbon trace of a RecA dimer taken from the crystal structure of the helical RecA protein filament (*6*). Subunit 1 is on the right (yellow α-carbon backbone) and subunit 2 is on the left (aqua α-carbon backbone). Highlighted areas include αA/*β*0 (green) and *β*3/αE (violet). Complementary interacting surfaces ($\alpha A_1/\beta 0_1$ with $\beta 3_2/\alpha E_2$) are in the center of the image. (B) Cross-subunit proximity of K6 (subunit 1)/D139 (subunit 2), and R28 (subunit 1)/D112/N113 (subunit 2). This image has been rotated 180° around the *y*-axis relative to the image in panel A.

following exposure to UV light or mitomycin C and were performed as previously described (*13*). Cell growth across a series of time zones of exposure was ranked from zero to 4, and fractional survival at 30 s was calculated from the slope of a line resulting from a plot of relative growth vs time. RecA-mediated cleavage of the LexA protein was measured using MacConkey-lactose plates as previously described (*13*).

Determination of the Oligomeric Properties of Mutant RecA Proteins. The effect of mutations on the oligomeric properties of RecA was determined by analyzing the elution profile of each protein on a Superose 6 HR gel filtration column as previously described (*17*). Column buffers contained 20 mM *β*ME. The concentration of RecA protein in the column load was always 26 *μ*M.

Electron Microscopy. Samples were prepared for electron microscopy by incubating wild-type or mutant RecA proteins at the indicated concentrations in the absence or presence of 3.0 *μ*M single-stranded circular DNA (*ϕ*X174 or RV-1). All reactions containing DNA included *E. coli* single-stranded DNA binding protein (0.03 *μ*M) and were preincubated at 37 °C for 5 min. Reaction buffer included 25 mM triethanolamine-HCl (pH 7.5), 50 mM KCl, 5 mM $MgCl_2$, 1 mM ATP*γ*S, and 5 mM *β*ME. Upon addition of RecA, reactions were incubated for 15 min at 37 °C. Reactions were spread onto thin carbon films on holey carbon grids (400 mesh) and stained with 1% uranyl acetate. Samples were visualized using a Philips CM10 electron microscope.

Gel Shift DNA Binding Assay. Reactions (30 *μ*L) were performed in a buffer containing 20 mM Tris-HCl (pH 7.5), 20 mM KCl, 10 mM $MgCl_2$, 0.5 mM EDTA, 0.5 mM ATP*γ*S, and 5 mM *β*ME. Reactions were initiated with addition of a 5'-end labeled 97 base oligonucleotide to a final concentration of 10 *μ*M (bases). Incubation was continued at 37 °C for 1 h followed by addition of glycerol to a final concentration of 12.5%. Samples were loaded onto a 1.2% agarose gel and electrophoresed in TAE buffer at 4 V/cm. Gels were analyzed using a Personal Molecular Imager FX and QuantityOne software (Bio-Rad).

ATPase Activity. Single-strand DNA-dependent hydrolysis of ATP was measured as described (*15*, *18*). Reaction buffer contained 2 mM DTT. PEI chromatography plates were analyzed using a Personal Molecular Imager FX and QuantityOne software (Bio-Rad).

Intersubunit Disulfide Cross-Links. Formation and analysis of intersubunit disulfide cross-links was performed as follows. Protein (50 *μ*g) was prereduced in the presence of 20 mM *β*ME (20 min, 22 °C) and desalted into reaction buffer (100 mM Tris-HCl, pH 8.5/0.1 mM EDTA/30 mM NaCl/15 mM $MgCl_2$/5% glycerol) using a Microcon concentrator (Amicon). Disulfide cross-links formed spontaneously by incubating protein (30 *μ*M final concentration) 60 min at 37 °C in the presence or absence of ATP*γ*S and/or ssDNA. NEM was added to a final concentration of 30 mM, followed immediately by addition of SDS to a final concentration of 1.0%. Previously, we showed that addition of NEM at this step is important for preventing formation of random disulfides when SDS is added (*19*). The reaction containing NEM was incubated for 10 min at 22 °C, Laemmli loading dye (-*β*ME) was added, and samples were electrophoresed on 8% SDS−polyacrylamide gels. Control experiments to ensure that all higher molecular weight bands observed on gels contained reducible disulfides were performed by incubating reactions with *β*ME (150 mM final concentration) following cross-linking. Gels were stained with Coomassie blue (R250), or Western blots were performed using poly-

Table 1: $C\beta_1-C\beta_2$ Cross-Subunit Distances between Indicated Residues

cross-subunit pair	$C\beta_1-C\beta_2$ distance (Å)
Lys6↔Asp139	9.6
Arg28↔Asp112	6.8
Arg28↔Asn113	6.3
Phe217↔Thr150	6.6

Table 2: In Vivo DNA Repair and Coprotease Activities

Cys mutant	fractional UV survival/30 s	survival in the presence of MMC (0.3/0.6 μg mL^{-1})	coprotease[a]
wild-type	1.00	1.00/1.00	i
6	0.75	1.00/0.75	i
28	1.00	1.00/1.00	c
112	1.00	1.00/1.00	i
113	1.00	1.00/1.00	i
139	1.00	1.00/0.85	i
6/139	0.75	0.75/0.75	i
28/112	1.00	1.00/0.75	c
28/113	1.00	1.00/0.75	c

[a] i indicates "inducible" activity in the presence of DNA damage. c indicates "constitutive" activity in the absence of DNA damage. All assays were repeated a minimum of four times and the range of standard errors is 5−15%.

clonal rabbit anti-RecA antibodies as previously described (*12*). Gels and blots were analyzed using a FluorS Multi-Imager (Bio-Rad). Reactions done in the presence of nucleotide cofactors contained either 1.0 mM ATP or 0.5 mM ATPγS. When present, single-stranded M13 DNA was added to a final concentration of 70 μM (nucleotides).

RESULTS

Design of Cys Mutations. The RecA crystal structure (*6*) shows that the N-terminal region of the protein, defined by α-helix A and β-strand 0 (residues 6−30), interacts with a region of the neighboring subunit defined by β-strand 3 and α-helix E (residues 111−140; Figure 1). The majority of the interactions between these two complementary surfaces are hydrophobic. Seven nonpolar side chains in subunit 1 are within van der Waals distance of eight nonpolar side chains in subunit 2. However, the structure shows that this large hydrophobic cluster is flanked by polar and ionic cross-subunit contacts. The ϵ-NH_3 group of Lys6 is 2.9 Å from one of the carboxylate oxygens of Asp139 in the neighboring subunit (Figure 1B). Also, one of the nitrogens in the guanidinium group of Arg28 (Nϵ) is 3.5 Å from the carbonyl oxygen of the Asn113 side chain (Figure 1B), and two of the nitrogens (Nϵ and Nη1) are within 3.0 Å of the main-chain carbonyl oxygen of Asp112. Double mutants were made with Cys at positions 6/139, 28/112, and 28/113. Single Cys mutants were also created at positions 6, 28, 112, 113, and 139. All mutant proteins could be overproduced and purified.

In Vivo Function of Mutant RecA Proteins. As shown in Table 2 all single and double Cys mutants maintain a high level of recombinational DNA repair function as measured by survival in the presence of mitomycin C or following exposure to UV irradiation. All proteins maintain 75% of wild-type recombination activity. All mutants also retained substantial levels of either inducible or constitutively activated coprotease function. These results demonstrate that each of the engineered Cys substitutions do not significantly impair RecA function.

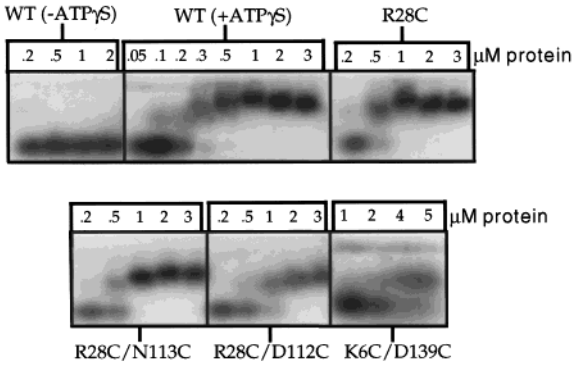

FIGURE 2: Gel shift DNA binding assays. Indicated concentrations of proteins were incubated with a 5'-end-labeled 97 base oligonucleotide and samples were electrophoresed on a 1.2% agarose gel. Reactions with wild-type RecA were done in the absence or presence of 0.5 mM ATPγS. Reactions with mutant proteins all contained 0.5 mM ATPγS.

Table 3: DNA Binding and ATPase Activities

Cys mutant	ssDNA binding $K_{D,app}$ (μM)[a]	V_i/E (mol ADP·min^{-1}·mol RecA^{-1})
wild-type	0.2	22.5
28	0.4	23.0
28/113	0.5	12.5
28/112	1.2	3.2
6/139	3.0	1.3

[a] $K_{D,app}$ was determined from plots of DNA bound vs protein concentration and represents the protein concentration at which 50% of substrate DNA is bound. DNA binding and ATPase assays were repeated three times and the standard errors approximated 20%.

Function of Mutant RecA Nucleoprotein Filaments. We tested the ability of each mutant protein to form catalytically active nucleoprotein filaments in vitro by assaying for DNA binding and ATPase activity. The gels in Figure 2 show that each protein maintains the ability to bind ssDNA although for the K6C/D139C mutant protein there is a substantial decrease in affinity. From plots of ssDNA bound vs RecA concentration (not shown) we estimate a $K_{D,app}$ of 0.2 μM for wild-type and 0.4 μM for the R28C single mutant (Table 3). Values of $K_{D,app}$ for the double mutants R28C/N113C, R28C/D112C, and K6C/D139C were estimated to be 0.5, 1.2, and 3.0 μM, respectively (Table 3). As for wild-type RecA, binding to ssDNA by all mutant proteins is dependent on the presence of ATP (or ATPγS).

Turnover numbers for the ssDNA-dependent ATPase activity were calculated for each protein (Table 3). For wild-type RecA and the R28C single mutant $V_i/E \approx 23.0$ mol ADP·min^{-1}·mol RecA^{-1}, whereas the double Cys mutant proteins showed varying degrees of inhibition with the K6C/D139C protein showing almost an 18-fold decrease in ATPase catalytic proficiency (Table 3).

Analyses of Oligomeric Properties. The oligomeric structure of the double Cys mutant proteins in both the presence and absence of ATP and ssDNA was analyzed by electron microscopy. In Figure 3 (panels A−D), we show negative stained electron micrographs of wild-type RecA and the 3 double Cys mutants in the presence of ATPγS. As seen previously (*20*−*23*), wild-type RecA forms a heterogeneous population of oligomeric structures including helical fila-

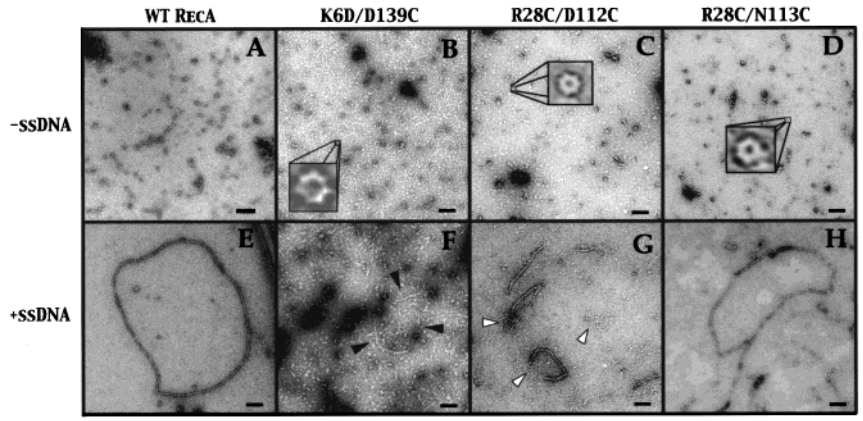

FIGURE 3: Negative stained electron micrographs of protein and protein-ssDNA complexes. Wild-type RecA and the three double Cys mutant proteins were incubated in the presence of 1.0 mM ATPγS and absence of ssDNA (A−D) or in the presence of 1.0 mM ATPγS and 3.0 μM phage circular ssDNA (E−H). Protein concentration in the absence of ssDNA (A−D) was 2.0 μM. Protein concentration in the presence of ssDNA for wild-type, R28C/D112C and R28C/N113C was 0.8 μM, while the concentration of K6C/D139C was 4.0 μM. White arrows in panel G indicate regions of ssDNA not bound by protein. Black arrows in panel F indicate the single nucleoprotein filament observed in this field. Black bar in each panel equals 0.1 μm.

ments that range in length from 0.03 to 0.15 μm. For the double Cys mutant proteins no filaments are observed indicating that each pair of Cys substitutions destabilizes subunit interactions that are important for extended polymerization in the absence of ssDNA. Although not shown in Figure 3, occasional longer filaments (~1.0 μm in length) were observed for the R28C/N113C protein in the presence of ATPγS, and these represented an extremely small percent of the total protein. These results are consistent with previous studies in which we showed that either a K6A or R28A substitution inhibited the stability of free protein filaments (*11*). Interestingly, all three double Cys mutant proteins form a significant amount of seven-membered ring shaped oligomers (Figure 3, inserts in panels B, C, and D).

In the presence of ssDNA and ATPγS, each double Cys mutant protein forms a nucleoprotein filament (Figure 3, panels F, G, and H), but the two that are most compromised in their DNA binding affinity (K6C/D139C, R28C/D112C) show distinct differences compared to wild-type RecA. As expected under the conditions used (0.8 μM protein, 3.0 μM bases of ssDNA), very little wild-type RecA remains in a free state and all DNA molecules with bound protein are fully covered, indicating cooperative filament formation by RecA on the ssDNA substrate (Figure 3E). The R28C/N113C mutant (Figure 3H) forms nucleoprotein filaments that look similar to those formed by wild-type RecA. The R28C/D112C mutant (Figure 3G) shows a defect in cooperative filament assembly on ssDNA as most of the DNA molecules with bound protein are only partially covered. Arrows in Figure 3G indicate regions of ssDNA not bound by protein. The K6C/D139C mutant has the lowest affinity for ssDNA (see above and Figure 2) and even at elevated protein concentrations (4.0 μM in Figure 3F) a significant percentage of the protein is not bound to ssDNA. Similar to the R28C/N112C mutant, the K6C/D139C nucleoprotein filaments that do form show regions of ssDNA not bound by protein. The helical pitch of nucleoprotein filaments formed by the mutant proteins is similar to that formed by wild-type RecA (~90−95 Å). Together, the functional and structural analyses show that despite defects in DNA binding affinity and cooperative filament assembly on ssDNA, cross-subunit disulfide formation between the engineered Cys residues in the mutant proteins should accurately reflect the position of these side chains in the catalytically active form of the RecA filament.

The oligomeric properties of the mutant proteins were also analyzed by gel filtration under conditions that closely matched those used in the disulfide cross-linking experiments, i.e., at protein concentrations ~30 μM. The Superose 6 profile in Figure 4A shows that wild-type RecA forms a heterogeneous mix of oligomers ranging from 5×10^6 Da to 68 kDa. In the presence of ATPγS, the oligomeric population undergoes a general shift to smaller sizes, a result that is consistent with previous studies using electron microscopy, light scattering, and gel filtration (*22*−*25*). In contrast, each of the mutant proteins shows a profile suggesting that the Cys mutations limit stable filament formation in either the absence or presence of ATPγS. The R28C/D112C protein retains some ability to form larger oligomers, and these shift to a smaller size in the presence of ATPγS. However, in this assay ATPγS does not show a significant effect on the oligomeric distribution of the K6C/D139C and R28C/N113C proteins.

Formation of Cross-Subunit Disulfide Bonds. Formation of cross-subunit disulfides was determined for each of the double Cys mutant proteins under three different conditions, in the absence of ATPγS and ssDNA, in the presence of ATPγS alone, and in the presence of both ATPγS and ssDNA. We found that the efficiency of disulfide formation was not affected by addition of oxidizing reagents; therefore, all disulfides observed in this study result from spontaneous cross-linking due to the proximity of the interacting Cys residues.

Cross-linking reactions were performed using the three double Cys mutant proteins (R28C/D112C, R28C/N113C, and K6C/D139C) and the resulting SDS−polyacrylamide gel run under nonreducing conditions is displayed in Figure 5. Monomeric RecA runs just beneath the 47.5 kDa marker, and disulfide formation between the engineered Cys substitutions results in a series of slower mobility bands. Judging by the staining intensity, the cysteines at positions 6 and 139 form a disulfide bond with greater efficiency than those at positions 28/112 or 28/113. This result was observed consistently during the course of this work. This is an unexpected result given that the $C\beta_1$-$C\beta_2$ distance between

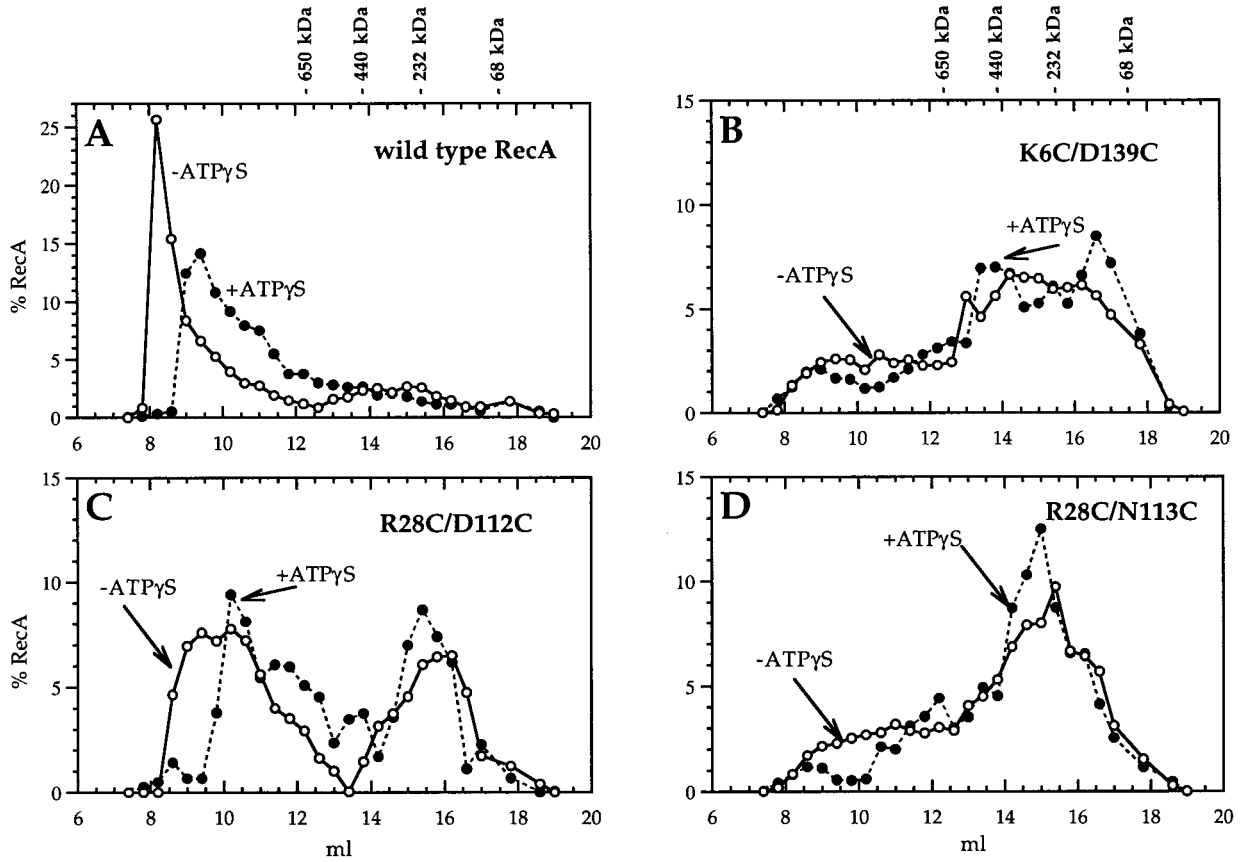

FIGURE 4: Gel filtration profiles of wild-type RecA and the three double Cys mutant proteins. Superose 6 gel filtration profiles reveal that the engineered Cys mutations inhibit formation of larger oligomeric species. Larger oligomers observed with wild-type RecA (A) and the R28C/D112C protein (C) undergo an ATP-induced shift to smaller sizes, whereas the oligomeric distribution of K6C/D139C (B) and R28C/N113C (D) is largely unaffected by the presence of ATP. Size markers are thyroglobulin (650 kDa), ferritin (440 kDa), catalase (232 kDa), and BSA (68 kDa).

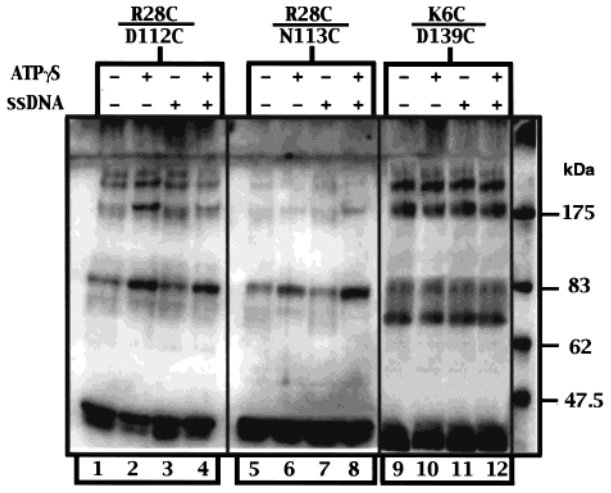

FIGURE 5: Disulfide cross-linking performed using the engineered double Cys mutant proteins. Proteins (30 μM) were incubated at 37 °C for 60 min in the absence or presence of ATPγS and ssDNA as indicated and processed as described in the Experimental Procedures. Monomeric RecA (38 kDa) runs near the bottom of the gel while slower mobility bands represent disulfide cross-linked dimers, trimers, etc. The efficiency of disulfide formation increases in the R28C/D112C and R28C/N113C proteins in the presence of either ATPγS or ATPγS/ssDNA.

residues 6 and 139 is 9.6 Å, whereas those between residues 28/112 and 28/113 are 6.8 and 6.3 Å, respectively (Table 1; see Discussion). Most interestingly, we find that both the R28C/D112C and R28C/N113C mutants show an increase in disulfide formation when cross-linking is done in the presence of ATPγS or ATPγS/ssDNA. ATPγS or ATPγS/ssDNA have no effect on the efficiency of disulfide formation in the K6C/D139C mutant. These data suggest that binding of ATPγS by RecA results in a conformational change that brings residues 28 and 112, as well as 28 and 113, into closer proximity, but does not significantly affect the proximity of residues 6 and 139 (see Discussion).

In previous work, we performed similar disulfide cross-linking between a F217C substitution and several engineered Cys mutations in the neighboring subunit (*19*). One double Cys mutant that was particularly efficient at disulfide formation was the F217C/T150C mutant. The gel in Figure 6 (lanes 4−6) shows that this mutant gives rise to a ladder of bands that extends well up into the gel well. During the time of cross-linking nearly all monomeric RecA is converted to higher molecular weight forms. The fact that the efficiency of disulfide formation does not correlate with the Cβ_1−Cβ_2 distances between residues 28/112, 28/113, and 217/150 (6.8 Å, 6.3 Å, and 6.6 Å, respectively; Table 1) suggests that cross-subunit distances seen in the RecA crystal structure may not accurately reflect those in the solution form of the RecA filament (see Discussion).

In a control experiment we show that none of the three native Cys residues in wild-type RecA formed disulfides that would interfere with our analyses of the cross-linking efficiency of the engineered Cys mutations (Figure 6, lanes 1−3). The X-ray structure of RecA also shows that none of

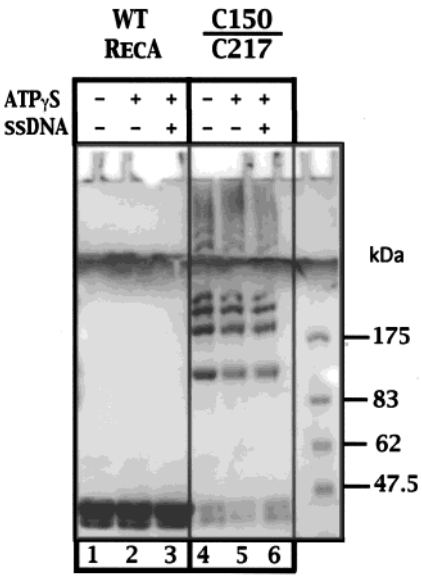

FIGURE 6: Disulfide cross-linking performed using wild-type RecA and the T150C/F217C mutant protein. Proteins (30 μM) were incubated at 37 °C for 60 min in the absence or presence of ATPγS and ssDNA as indicated and processed as described in the Experimental Procedures. The three Cys residues in wild-type RecA do not show any disulfide formation that results in subunit cross-linking while the T150C/F217C mutant protein shows very efficient formation of cross-subunit disulfides that is not affected by the presence of either ATPγS or ATPγS/ssDNA.

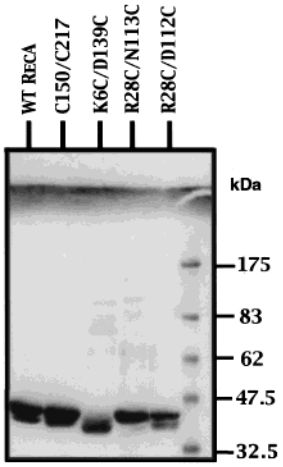

FIGURE 7: Disulfide cross-linking followed by incubation with βME. Disulfide cross-linking experiments were performed as described (Experimental Procedures) followed by incubation with βME (150 mM). All proteins migrate at the position of monomeric RecA and show no slower mobility bands.

the three native cysteine side chains are close enough to form a disulfide with cysteines introduced at positions 6, 28, 112, 113, or 139 (not shown). Therefore, although previous work has shown that none of the native Cys residues is critical for RecA function (*26*), we chose not to mutate these in order to avoid any further compromise to the structural and functional integrity of the designed mutant proteins in this study.

Additional controls included cross-linking reactions with each protein followed by incubation with excess βME. Samples were run on an SDS gel under reducing conditions and the results in Figure 7 show that all proteins migrate as a single band at the position of monomeric RecA. This demonstrates that the slower mobility bands in Figures 5 and 6 result exclusively from formation of cross-subunit disulfides between the engineered Cys residues in the mutant proteins.

DISCUSSION

In this study, we provide direct biochemical evidence for an ATP-induced movement of specific side chains within the subunit interface of the RecA protein. In the RecA crystal structure, Arg28 is close to both Asp112 and Asn113 in the neighboring subunit (Figure 1). Formation of a specific cross-subunit disulfide bond results when pairwise Cys substitutions are introduced at positions 28 and 112, or positions 28 and 113, and in both cases, the efficiency of disulfide formation is increased in the presence of ATPγS or ATPγS/ssDNA. We performed a series of assays to assess the effects of the designed Cys mutations on both the functional and structural properties of RecA, and based on these we conclude that the observed changes in disulfide formation reflect a genuine ATP-induced reorientation of these positions in the wild-type protein. First, in vivo analyses of recombination proficiency show that all single and double Cys mutants maintain at least 75% of wild-type RecA function (Table 2). Second, the three double Cys mutant proteins maintain both an ATP-dependent ssDNA binding activity as well as a DNA-dependent ATPase activity, although the K6C/D139C mutant shows a significant decrease in both functions (Table 3). Third, electron microscopic analyses reveal that each of the three double Cys mutant proteins forms a nucleoprotein filament with dimensions, e.g. diameter and pitch, virtually identical to wild-type RecA, despite the fact that the R28C/D112C and K6C/D139C proteins show a defect in cooperative filament assembly on ssDNA. The fact that the K6C/D139C protein does show some level of in vivo and in vitro function eliminates the possibility that no ATP-induced change in disulfide cross-linking is seen simply because the protein does not bind ATP.

The helical filaments formed by RecA in either the absence or presence of ATP and DNA have distinct structural parameters. This has been most clearly demonstrated by electron microscopy (reviewed in refs *27* and *28*) and additionally with the use of hydrodynamic and biochemical methods (*24*, *29*). EM reconstructions reveal that filaments formed in the absence of any cofactor (the "inactive" form) have ~6.1 subunits/helical turn and a pitch of 76 Å, while filaments formed in the presence of ATPγS (or ADP−AlF_4) and DNA (the "active" form) have ~6.2 subunits/helical turn and a pitch of 95 Å (*27*). In the RecA crystal structure, the protein filament has 6.0 subunits/turn and a pitch of 82.7 Å in the absence of cofactors (*6*) and 83.1 Å in the presence of ADP (*30*). Therefore, there must be some differences in the arrangement of amino acid side chains at the subunit interface when comparing the crystal structure with EM reconstructions of the active filament form. Ideally, for these Cys cross-linking studies, we would like to compare the efficiency of disulfide formation in the inactive vs active form of the filament. In fact, in our earlier work mutant proteins carrying a F217C substitution and another Cys substitution on the surface of the neighboring subunit were able to form both catalytically active nucleoprotein filaments as well as inactive filaments in the absence of ATPγS and DNA (*19*). In the present study, each of the double Cys

mutants can form a catalytically active nucleoprotein filament yet formation of filaments in the absence of ATPγS and DNA is limited, even at protein concentrations used in the cross-linking reactions ($\sim$30 μM). At this higher protein concentration the oligomeric distribution of the R28C/D112C protein is shifted to smaller sizes upon incubation with ATPγS, and this may contribute in part to the observed ATP-induced changes in the efficiency of disulfide formation. However, ATPγS does not significantly affect the oligomeric distribution of the R28C/N113C protein and the observed increase in disulfide formation with this protein is most simply explained by an ATP-induced conformational change occurring within each RecA subunit that adjusts the cross-subunit proximity of residues 28 and 113. Given the heterogeneity of the oligomeric population for all three mutant proteins in the absence of ATP and DNA at the concentrations used in the cross-linking experiments (Figure 4), we are not strictly comparing the efficiency of disulfide formation between the inactive vs active filament forms of each protein. However, our data does indicate that conformational changes at the subunit interface induced by binding of ATPγS and ATPγS/ssDNA can be monitored by changes in the efficiency of disulfide formation between the engineered Cys residues.

The acceptable limits for Cβ_1−Cβ_2 distances in disulfide bonds is 2.9−4.6 Å as determined by measurements of disulfides in protein structures and by modeling (*31*, *32*). Although the Cβ_1−Cβ_2 distance for each pair of residues in this study (6.3−9.6 Å) is greater than 4.6 Å, clearly the Cys substitutions introduced at positions 6/139, 28/112, and 28/113 are close enough to result in some degree of disulfide formation. Interestingly, the Cβ_1−Cβ_2 distances and the orientation of the side chains for these three pairs in the crystal structure would predict the following order for the efficiency of disulfide cross-linking: 28/113 > 28/112 > 6/139. In fact, exactly the opposite is observed. The K6C/D139C protein shows the greatest amount of disulfide formation despite the fact that the Cβ_1−Cβ_2 distance of 9.6 Å is $\sim$3 Å greater than the other pairs. However, given the flexibility of the extreme N-terminal region of RecA (crystallographic B-factors for all atoms at positions 3−7 are $\geq$52.4 Å^2), Cys substitutions at residues 6 and 139 likely spend more time within bonding distance than is indicated by the Cβ_1−Cβ_2 distance in the structure. The Cβ_1−Cβ_2 distance for the 28/112 pair is 0.5 Å greater than 28/113, and the crystal structure shows that the N113 side chain is directed toward the subunit interface and R28, while D112 is directed more inward toward its own subunit (Figure 1). However, the 28/112 pair consistently cross-links with greater efficiency than the 28/113 pair. Additionally, the F217C/T150C mutant protein forms an intersubunit disulfide very efficiently (Figure 6 and ref *19*) yet has a Cβ_1−Cβ_2 distance intermediate between the 28/112 and 28/113 pairs (Table 1). Therefore, the Cβ_1−Cβ_2 distances derived from the crystal structure do not necessarily correspond to the observed efficiency of disulfide formation. While we certainly recognize that the oligomeric defects resulting from the paired Cys mutations at positions 6/139, 28/112 and 28/113 may play a role in the unexpected "reverse" order of cross-linking (see Figures 3 and 4), the results also suggest that the crystal structure may not accurately display the relative distances between these side chains as they occur in the solution structure of the protein.

The "head-to-tail" polymeric arrangement of the RecA protein filament creates a rather complex mixture of surfaces that make up the subunit interface. In our studies of different regions of the interface, we have attempted to identify two general classes of cross-subunit interactions, those that are important for stabilization of the protein oligomeric structure and those that are involved in the transmission of allosteric information across the interface. Of course, these two classes are not necessarily mutually exclusive. Recently, we have demonstrated that Phe217, which lies in another area of the subunit interface, plays a direct role in transmitting ATP-induced allosteric information throughout the RecA filament (*33*). Analysis of the oligomeric properties of various mutant proteins with substitutions at position 217 suggest that this residue is less important for the overall stabilization of the RecA filament, rather its primary role is in allosteric information transfer (*17*, *33*). However, other residues in this same area do play important roles in stabilizing the oligomeric structure of the protein (*17*). The region of the subunit interface that is the focus of the present study appears to be involved exclusively in stabilizing the filament structure of RecA and is unlikely to play any direct role in the transmission of allosteric information. Several pieces of evidence support this idea. Mutant proteins carrying a F217C substitution paired with various other Cys mutations on the surface of the neighboring subunit form disulfide cross-links but show no ATP-induced change in the efficiency of disulfide formation (*19*). In contrast, ATP does change the efficiency of disulfide formation between pairs of Cys substitutions at positions 28/112 and 28/113. Additionally, a conservative F217Y mutation increases ATP-mediated cooperative filament assembly >250-fold (*33*). Together these data are consistent with the idea that it is Phe217 that mediates ATP-induced shifts in the positions of residues at the subunit interface and that residues 28, 112, and 113 are not involved in this signaling process. This idea is also supported by results from Zaitsev and Kowalczykowski (*34*) in which they showed that the *recA*$^-$ phenotype of a *recA*Δ9 mutant (a truncation that removes the first nine residues) is suppressed by a second site mutation that apparently increases the stability of cross-subunit interactions in this area of the interface. Therefore, in the wild-type protein any cross-subunit interactions mediated by residues 1−9 and their partners on the neighboring surface, e.g. Lys6↔Asp139, cannot play important roles in a mechanistic process involving allosteric information transfer.

Further studies are aimed at clarifying molecular interactions within various areas of the RecA subunit interface and how they contribute to stable assembly of RecA filaments and optimization of catalytic function.

ACKNOWLEDGMENT

The authors wish to thank Dr. Celia Schiffer for help with creating Figure 1 and Dr. Julie DeZutter and Janice Lloyd for valuable discussions.

REFERENCES

1. Radding, C. M. (1989) *Biochim. Biophys. Acta 1008*, 131−145.

2. Eggleston, A. K., and West, S. C. (1996) *Trends Genet. 12*, 20−26.
3. Roca, A. I., and Cox, M. M. (1997) *Prog. Nucl. Acid Res. Mol. Biol. 56*, 129−222.
4. Bianco, P. R., Tracy, R. B., and Kowalczykowski, S. C. (1998) *Front. Biosci. 3*, D570−D603.
5. De Zutter, J. K., and Knight, K. L. (1999) *J. Mol. Biol. 293*, 769−780.
6. Story, R. M., Weber, I. T., and Steitz, T. A. (1992) *Nature 355*, 318−325.
7. Yarranton, G. T., and Sedgewick, S. G. (1982) *Mol. Gen. Genet. 185*, 99−104.
8. Kiselev, V. I., Glukhov, A. I., Tarasova, I. M., and Shchepetov, M. E. (1988) *Mol. Biol. (Mosk) 22*, 1198−1203.
9. Mikawa T., Masui R., Ogawa T., Ogawa H., and Kuramitsu S. (1995) *J. Mol. Biol. 250*, 471−483.
10. Masui, R., Mikawa, T., and Kuramitsu, S. (1997) *J. Biol. Chem. 272*, 27707−27715.
11. Eldin, S., Forget, A. L., Lindenmuth, D., Logan, K. M., and Knight, K. L. (2000) *J. Mol. Biol. 299*, 91−101.
12. Logan, K. M., and Knight, K. L. (1993) *J. Mol. Biol. 232*, 1048−1059.
13. Nastri, H. G., and Knight, K. L. (1994) *J. Biol. Chem. 269*, 26311−26322.
14. Levinson, A., Silver, D., and Seed, B. (1984) *J. Mol. Appl. Genet. 2*, 507−517.
15. Konola, J. T., Nastri, H. G., Logan, K. M., and Knight, K. L. (1995) *J. Biol. Chem. 270*, 8411−8419.
16. Skiba, M. C., and Knight, K. L. (1994) *J. Biol. Chem. 269*, 3823−3828.
17. Logan, K. M., Skiba, M. C., Eldin, S., and Knight, K. L. (1997) *J. Mol. Biol. 266*, 306−316.
18. Weinstock, G. M., McEntee, K., and Lehman, I. R. (1981) *J. Biol. Chem. 256*, 8829−8834.
19. Skiba, M. C., Logan, K. M., and Knight, K. L. (1999) *Biochemistry 38*, 11933−11941.
20. DiCapua, E., Engel, A., Stasiak, A., and Koller, Th. (1982) *J. Mol. Biol. 157*, 87−103.
21. Egelman, E. H., and Stasiak, A. (1988) *J. Mol. Biol. 200*, 329−349.
22. Brenner, S. L., Zlotnik, A., and Griffith, J. D. (1988) *J. Mol. Biol. 204*, 959−972.
23. Heuser, J., and Griffith, J. (1989) *J. Mol. Biol. 210*, 473−484.
24. Wilson, D. H., and Benight, A. S. (1990) *J. Biol. Chem. 265*, 7351−7359.
25. Ruigrok, R. W. H., and DiCapua, E. (1991) *Biochimie 73*, 191−197.
26. Weisemann, J. M. and Weinstock, G. M. (1988) *DNA 7*, 389−398.
27. Egelman, E. H., and Stasiak, A. (1993) *Micron 24*, 309−324.
28. Egelman, E. H. (1993) *Curr. Opin. Struct. Biol. 3*, 189−197.
29. Kobayashi, N., Knight, K. L., and McEntee, K. (1987) *Biochemistry 26*, 6801−6810.
30. Story, R. M., and Steitz, T. A. (1992) *Nature 355*, 374−376.
31. Hazes, B., and Dijkstra, B. W. (1988) *Protein Eng. 2*, 119−125.
32. Sowdhamini, R., Srinivasan, N., Shoichet, B., Santi, D. V., Ramakrishnan, C., and Balaram, P. (1989) *Protein Eng. 3*, 95−103.
33. De Zutter, J. K., Forget, A. L. Logan, K. M., and Knight, K. L. (2001) *Structure 9*, 47−55.
34. Zaitsev, E. N., and Kowalczykowski, S. C. (1999) *Mol. Microbiol. 34*, 1−9.

BI011081U